

# Electrical resistivity and thermopower measurements of the hole- and electron-doped cobaltites $LnCoO_3$

Z. Jiráček, J. Hejtmánek, K. Knížek, and M. Veverka

*Institute of Physics, Cukrovarnická 10, 162 53 Prague 6, Czech Republic*

(Received 28 April 2008; revised manuscript received 17 June 2008; published 31 July 2008)

Two perovskite cobaltites,  $LaCoO_3$  and  $DyCoO_3$ , which are border compounds with respect to the  $Ln$  size, were investigated by the electric resistivity and thermopower measurements up to 800–1000 K. Special attention was given to effects of extra holes or electrons, introduced by light doping of Co sites by  $Mg^{2+}$  or  $Ti^{4+}$  ions. The experiments on the La-based compounds were complemented by magnetic measurements. The study shows that both kinds of charge carriers induce magnetic states on surrounding  $Co^{3+}$  sites and form thus thermally stable polarons of large total spin. Their itinerancy is characterized by low-temperature resistivity, which is of Arrhenius type  $\rho \sim \exp(E_A/kT)$  for the hole ( $Co^{4+}$ )-doped samples, while an unusual dependence  $\rho \sim 1/T^n$  ( $n=8-10$ ) is observed for the electron ( $Co^{2+}$ )-doped samples. At higher temperatures, additional hole carriers are massively populated in the  $Co^{3+}$  background, leading to a resistivity drop. This transition becomes evident at  $\sim 300$  K and 450 K and culminates at  $T_{I-M}=540$  and 780 K for the La- and Dy-based samples, respectively. The electronic behaviors of the cobaltites in dependence on temperature are explained considering local excitations from the diamagnetic low-spin (LS)  $Co^{3+}$  to close-lying paramagnetic high-spin (HS)  $Co^{3+}$  states and subsequent formation of a metallic phase of the IS  $Co^{3+}$  character through a charge transfer mechanism between LS/HS pairs. The magnetic polarons associated with doped carriers are interpreted as droplets of such intermediate (IS) phase.

DOI: [10.1103/PhysRevB.78.014432](https://doi.org/10.1103/PhysRevB.78.014432)

PACS number(s): 74.25.Ha, 71.30.+h, 75.30.Wx

## I. INTRODUCTION

The nature of spin-state transitions in perovskite cobaltite  $LaCoO_3$  and its rare-earth analogs are under debate for decades. Early work of Heikes, Miller, and Mazelsky in 1964 (Ref. 1) on the electric transport properties of  $LaCoO_3$  revealed an existence of the insulator-metal transition at  $T_{I-M}=540$  K, and the effective magnetic moments derived from susceptibility measurements led to a tentative conclusion that the room-temperature semiconducting phase is based on  $Co^{3+}$  ions in the intermediate-spin (IS,  $t_{2g}^5 e_g^1$ ,  $S=1$ ) state, while the high-temperature metallic phase is of a mixed, intermediate-spin, and high-spin (HS,  $t_{2g}^4 e_g^2$ ,  $S=2$ ) character. The high conduction of this phase was ascribed to mobile carriers generated through the dynamic  $Co^{2+}/Co^{4+}$  charge excitation. Experiments performed down to liquid helium temperature showed shortly later that the true ground state is diamagnetic, based on the low-spin (LS,  $t_{2g}^6 e_g^0$ ,  $S=0$ ) state of  $Co^{3+}$  ions, and the origin of the room-temperature paramagnetism was ascribed to thermal population of close-lying high-spin states, which develops progressively at  $T_{magn}=80$  K [see, e.g., Raccach and Goodenough 1967 (Ref. 2)]. The existence of IS states was thus questioned and the room-temperature phase was reinterpreted as a mixture of LS and HS  $Co^{3+}$  states in ratio approaching 1:1.

Nowadays, there is no doubt about the LS ground state of  $LaCoO_3$  and the gradual population of paramagnetic  $Co^{3+}$  states through the thermal excitation, but remains controversy concerning their IS or HS nature. The prevailing interpretation assumes that the paramagnetic states populated at low temperatures are of the IS kind, while the HS states become excited at elevated temperatures—the LS  $\rightarrow$  IS  $\rightarrow$  HS scenario. In the high-temperature limit, the thermodynamic equilibrium is obtained for a mixture of all three  $Co^{3+}$

spin states, and the population of orbitally and spin-degenerated IS and HS states finally dominates over the LS singlet states. Several experimental findings are quoted in favor of this scenario: The magnetic susceptibility and anomalous expansion data can be fitted well within simple Boltzmann statistics of independent excitations.<sup>3,4</sup> Local distortions, observed at low temperatures by the diffraction and spectroscopic [x-ray absorption near-edge spectroscopy (XANES)] methods, can be related to presence of Jahn-Teller active IS states.<sup>5</sup> The spin density distribution, probed by the polarized neutron diffractometry on the  $LaCoO_3$  crystal in strong magnetic field, is also suggesting for the IS states.<sup>6</sup> The low-temperature IS excitations are reported also in numerous photoemission and x-ray absorption spectroscopic studies, while the presence of HS states at the first stages of the diamagnetic-paramagnetic transition have been disproved based on the theoretical simulations (see, e.g., Ref. 7).

Alternative interpretation associates the transition at  $T_{magn}=80$  K with the HS excitations. Among recent experiments, the most direct evidence comes from electron spin resonance (ESR) experiments on  $LaCoO_3$  of Noguchi *et al.*<sup>8</sup> The study shows that the first excited state is pseudotriplet  $J=1$  with effective value  $g=3.35$ . This finding is in striking agreement with properties of the spin-orbit split  $^5T_{2g}$  term of  $3d^6$  ions ( $Fe^{2+}$ ,  $Co^{3+}$ ) in octahedral crystal field (see, e.g., Refs. 9 and 10) and provides a strong evidence that at least up to 50 K before the ESR signal becomes unobservable, the excited  $Co^{3+}$  states are of the HS nature. At higher temperatures, only indirect arguments for the LS/HS coexistence are available, e.g., the detection of an important spin-orbit coupling, characteristic for HS state, in studies of inelastic neutron scattering and x-ray magnetic circular dichroism.<sup>10,11</sup> Based on these experimental findings and extensive LDA

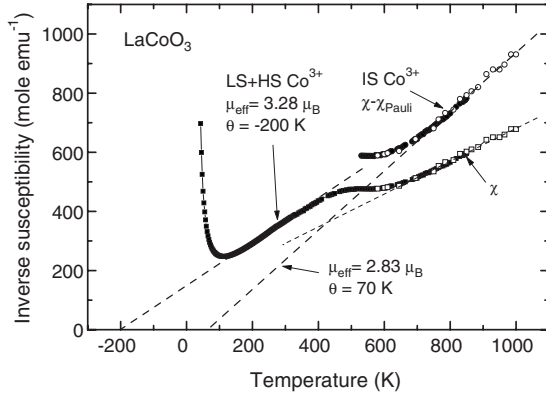


FIG. 1. The inverse susceptibility in LaCoO<sub>3</sub>, demonstrating two regions of Curie-Weiss behavior. The squares refer to the measured susceptibility while circles are obtained by subtraction of the Pauli temperature-independent term  $\chi_o \sim 0.0004$  emu/mol. Open symbols are data taken from Ref. 15

+U and Hartley-Fock theoretical calculations,<sup>12,13</sup> we doubt about the existence of IS states at the low-temperature region and incline to the early model of Goodenough of the room-temperature LaCoO<sub>3</sub> phase as a dynamic LS/HS mixture with HS excitations conditioned by the presence of LS states at the nearest neighbors.<sup>14</sup> In our opinion, this nonuniform LS/HS phase is gradually transformed, with a center at  $T_{I-M} = 540$  K, to the homogeneous IS phase. We relate the apparent discrepancy between the theoretical effective moment for IS state,  $\mu_{\text{eff}} = 2.83 \mu_B$ , and the frequently reported experimental value  $\mu_{\text{eff}} = 3.90 \mu_B$  to an uncorrected effect of significant Pauli susceptibility present in the high-temperature metallic phase (see Fig. 1 with our data and data taken from Ref. 15). The value of  $\chi_o \sim 0.0004$  emu mol<sup>-1</sup>, derived in a least-squares fit, suggests that density of states at the Fermi level of the IS phase of LaCoO<sub>3</sub> is about 170 Ryd<sup>-1</sup> per formula unit (in the free-electron approximation). Interestingly, this value matches quite well with the density of states 250 Ryd<sup>-1</sup>, determined for ferromagnetic metallic cobaltites La<sub>1-x</sub>Sr<sub>x</sub>CoO<sub>3</sub> ( $x \geq 0.5$ ) from

observed low-temperature electronic specific heat,  $\gamma \sim 0.043$  J mol<sup>-1</sup> K<sup>-2</sup>.<sup>16</sup>

The same LS  $\rightarrow$  HS  $\rightarrow$  IS scenario is applicable also for rare-earth systems  $Ln\text{CoO}_3$ . Some distinction appears due to a fast shift of the paramagnetic transition with decreasing  $Ln$  size to higher temperatures so that the I-M transition develops without previous saturation of the LS/HS phase. In particular for DyCoO<sub>3</sub> the transitions develop practically concurrently,  $T_{\text{magn}} = 740$  K,  $T_{I-M} = 780$  K.<sup>17</sup>

In this paper, we present the electrical transport properties of two extreme members of the cobaltite series, LaCoO<sub>3</sub> and DyCoO<sub>3</sub>, and investigate the role of extra holes or electrons that are introduced by light doping of Co sites by nonmagnetic Mg<sup>2+</sup> or Ti<sup>4+</sup> ions. It appears that both kinds of charge carriers induce magnetic states on surrounding LS Co<sup>3+</sup> sites and form thus a sort of magnetic polaron of a large total spin. Consistently with the above mentioned scenario, the polarons are interpreted as droplets of the IS phase that move in the background of the low-temperature LS or LS/HS phases of undoped  $Ln\text{CoO}_3$  and are finally dissolved in the high-temperature IS phase of the host.

II. EXPERIMENT

The ceramic samples LaCo<sub>1-x</sub>M<sub>x</sub>O<sub>3</sub> and DyCo<sub>1-x</sub>M<sub>x</sub>O<sub>3</sub> ( $x = 0, 0.02, \text{ and } 0.05, M = \text{Ti}^{4+}, \text{Mg}^{2+}$ ) have been prepared by solid state reaction at high temperatures. The mixtures of respective oxides in stoichiometric proportions were calcined at 800–900 °C. The powder was then homogenized, pressed into the form of pellets, and sintered at 1300 °C (for Mg compound at 1200 °C) for 40–60 h in air. The powder x-ray patterns of the products were recorded by using a Bruker D8 diffractometer with CuK $\alpha$  radiation. The LaCo<sub>1-x</sub>M<sub>x</sub>O<sub>3</sub> samples were of a single perovskite phase of the rhombohedral  $R\bar{3}c$  symmetry. The DyCo<sub>1-x</sub>M<sub>x</sub>O<sub>3</sub> samples showed perovskite phase of the orthorhombic  $Pbnm$  symmetry. Traces of impurity were detected for nominal composition DyCo<sub>0.95</sub>Mg<sub>0.05</sub>O<sub>3</sub>, pointing to a limited range of possible Mg doping. The lattice parameters obtained by the Rietveld fit are summarized in Table I.

TABLE I. Lattice parameters for LaCo<sub>1-x</sub>M<sub>x</sub>O<sub>3</sub> and DyCo<sub>1-x</sub>M<sub>x</sub>O<sub>3</sub>.

LaCo <sub>1-x</sub> M <sub>x</sub> O <sub>3</sub>	x	a (Å)	c (Å)	$\alpha_{\text{rhom}}$	V/Z (Å <sup>3</sup> )
	0	5.442(1)	13.194(2)	60.79(1)	55.97(1)
Ti	0.02	5.445(1)	13.114(1)	60.78(1)	56.07(1)
Ti	0.05	5.446(1)	13.111(2)	60.80(1)	56.09(1)
Mg	0.02	5.444(1)	13.199(1)	60.79(1)	56.03(1)
Mg	0.05	5.444(1)	13.111(1)	60.78(1)	56.05(1)
DyCo <sub>1-x</sub> M <sub>x</sub> O <sub>3</sub>	x	a (Å)	b (Å)	$c/\sqrt{2}$ (Å)	
	0	5.168(1)	5.418(1)	5.228(1)	51.67(1)
Ti	0.02	5.169(1)	5.411(1)	5.229(1)	51.71(1)
Ti	0.05	5.171(1)	5.413(1)	5.231(1)	51.75(1)
Mg	0.02	5.169(1)	5.411(1)	5.229(1)	51.69(1)

The low-temperature measurements of the electrical resistivity and thermoelectric power were carried out between 10–310 K using a close-cycle He refrigerator. For the high-temperature measurements the sample was placed on the ceramic sample holder centered in the small tubular furnace with precisely controlled temperature. The standard  $K$ -type thermocouples (chromel–alumel) were used for the monitoring of the temperature gradient around 5 K, imposed across the sample by means of an additional small furnace. In both the low- and high-temperature measurements, the four-point steady state method for resistivity and thermopower was applied.

Auxiliary magnetic susceptibility data were obtained by measurements in constant field of 1 T.

### III. RESULTS

#### A. The hole- and electron-doped systems $\text{LaCo}_{1-x}\text{M}_x\text{O}_3$ , $\text{M}=\text{Mg}^{2+}$ , and $\text{Ti}^{4+}$

The low-temperature conduction in the undoped  $\text{LnCoO}_3$  compounds is associated with extra carriers present due to weak nonstoichiometry. Generally, the carriers are of the hole character,  $n_h \leq 0.001/\text{Co}$  ( $\sim 10^{19} \text{ cm}^{-3}$ ), according to observed  $p$ -type thermopower and Hall effect. Additional hole carriers, thermally excited, become dominant in the high-temperature region. The excitation process accelerates due to the gradual closing of the charge transfer gap. The density of charge carriers as high as  $n_h \sim 1/\text{Co}$  ( $\sim 10^{22} \text{ cm}^{-3}$ ) for  $\text{LaCoO}_3$  above 540 K is reported.<sup>18</sup>

The concentration of holes in the low-temperature region can be effectively controlled by a light substitution of divalent Ca, Sr, and Ba cations on the  $\text{Ln}$  sites or, in present case, by substitutions of  $\text{Mg}^{2+}$  cations on the Co sites. Figure 2 compares transport properties of two nominally single-valent  $\text{Co}^{3+}$  cobaltites ( $\text{LaCoO}_3$ ,  $\text{LaCo}_{0.95}\text{Ga}_{0.05}\text{O}_3$ ) and some mixed valency  $\text{Co}^{3+}/\text{Co}^{4+}$  systems with divalent substitutions ( $\text{LaCo}_{0.98}\text{Mg}_{0.02}\text{O}_3$ ,  $\text{LaCo}_{0.95}\text{Mg}_{0.05}\text{O}_3$ ,  $\text{La}_{0.99}\text{Sr}_{0.01}\text{CoO}_3$ , and  $\text{La}_{0.98}\text{Sr}_{0.02}\text{CoO}_3$ ). The evident feature is a tendency of the resistivity and thermopower values to saturate around the room temperature, i.e., below temperatures where the massive population of carriers in  $\text{LaCoO}_3$  starts. The observed Seebeck coefficient  $\alpha_{300 \text{ K}} = +700 \mu\text{VK}^{-1}$  for the two  $\text{Co}^{3+}$  systems gives an estimate  $n_h = 0.0005/\text{Co}$  when the classical Heikes formula for thermopower in the hopping regime is applied [ $\alpha_{h,e} = \pm (k/e) \ln\{(1-n_{h,e})/n_{h,e}\}$  for hole and electron carriers, respectively]. Similarly, the plateaux  $\alpha \sim +400 \mu\text{VK}^{-1}$  observed at 150–350 K for  $\text{LaCo}_{0.98}\text{Mg}_{0.02}\text{O}_3$  and  $\text{LaCo}_{0.95}\text{Mg}_{0.05}\text{O}_3$  points to the identical concentration of hopping holes ( $\text{Co}^{4+}$  ions) of about  $n_h = 0.01/\text{Co}$ , irrespective the different Mg dopings. The apparent activation energy defined as  $E_A = k \cdot d(\ln \rho) / d(1/T)$ , i.e., anticipating Arrhenius-type formula  $\rho \sim \exp(E_A/kT)$  for the low-temperature transport, is shown in the inset of Fig. 2. The derived  $E_A$  values tend to zero in the LS ground state and attain a maximum of about 50 meV at about 80 K. The I-M transition is visualized as a huge peak in the apparent activation energy, centered at 500 K for all  $\text{LaCo}_{1-x}\text{M}_x\text{O}_3$  samples. It is worth mentioning that this temperature reflects likely an onset of percolation of the metallic phase rather than the true middle of the metallic

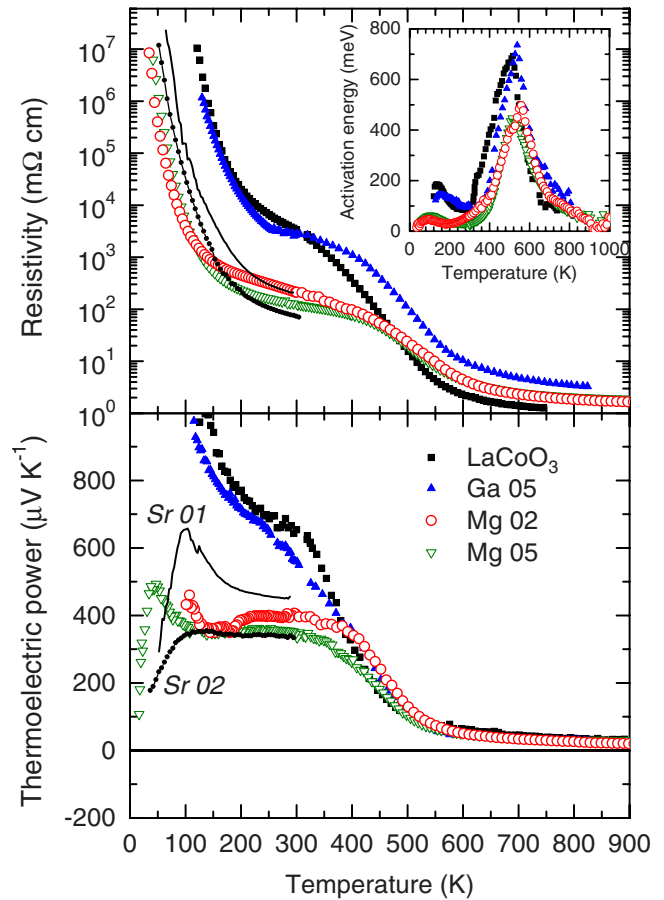


FIG. 2. (Color online) Electric resistivity and thermopower for  $p$ -type  $\text{LaCoO}_3$ ,  $\text{LaCo}_{0.95}\text{Ga}_{0.05}\text{O}_3$ ,  $\text{LaCo}_{0.98}\text{Mg}_{0.02}\text{O}_3$ , and  $\text{LaCo}_{0.95}\text{Mg}_{0.05}\text{O}_3$ . The lanthanum site substituted systems  $\text{La}_{0.99}\text{Sr}_{0.01}\text{CoO}_3$  and  $\text{La}_{0.98}\text{Sr}_{0.02}\text{CoO}_3$  are added for comparison. The inset of upper panel shows an apparent activation energy defined as  $E_A = k \cdot d(\ln \rho) / d(1/T)$ .

phase formation at  $T_{I-M} = 540 \text{ K}$ , reported, e.g., in the anomalous expansion experiments.<sup>17</sup>

The transport properties at the highest temperatures are characterized by a continuous decrease in the apparent activation energy. At the same temperatures, the thermopower still decreases in a hyperbolic ( $1/T$ ) way, demonstrating that closing of the charge transfer gap continues for temperatures even well above the apparent width of the I-M transition. This may signify certain phase-separated state, where metallic IS phase coexists with residual regions of the mixed LS/HS character.

Selected  $\text{LaCo}_{1-x}\text{M}_x\text{O}_3$  samples have been further characterized by susceptibility measurements. As shown in Fig. 3, the observed temperature dependence of susceptibility can be separated into two components—first one is the magnetic background of pure  $\text{LaCoO}_3$ , which reflects the spin-state transitions at  $T_{\text{magn}} = 80 \text{ K}$  and  $T_{I-M} = 540 \text{ K}$ , and second one is a simple Curie-type contribution,  $\chi_C = C/T$ , which is responsible for the low-temperature tail of susceptibility and persists obviously up to high temperatures (for more details see also Ref. 19). The Curie-type contribution is small for the  $\text{Ga}^{3+}$ -doped system  $\text{LaCo}_{0.95}\text{Ga}_{0.05}\text{O}_3$  and pure  $\text{LaCoO}_3$ , and is much enhanced for compounds doped on Co sites by het-

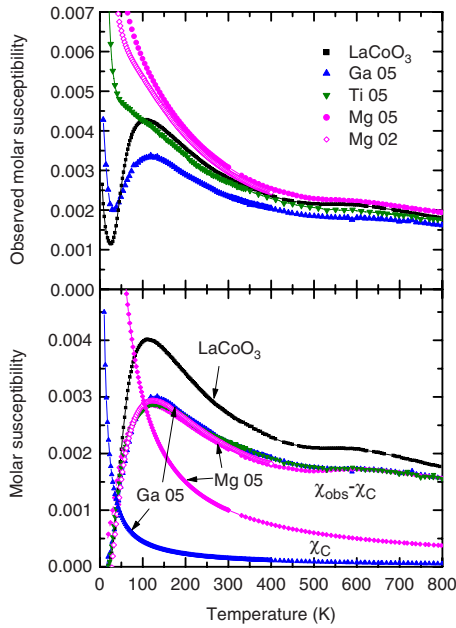


FIG. 3. (Color online) The measured magnetic susceptibility on  $\text{LaCoO}_3$  and some Co site substituted samples. Lower panel shows a separation into two components, one of which is taken as a simple Curie term,  $\chi_C = C/T$  (plotted here for  $\text{LaCo}_{0.95}\text{Gd}_{0.05}\text{O}_3$  and  $\text{LaCo}_{0.95}\text{Mg}_{0.05}\text{O}_3$  only). It appears that the susceptibility data after subtraction of this term merge together and show the same anomalies as undoped  $\text{LaCoO}_3$ .

erivalent  $\text{Mg}^{2+}$  and  $\text{Ti}^{4+}$  ions, suggesting that this additional magnetic term arises due to extra carriers in the cobaltites. When the Curie-type contribution observed for  $\text{LaCo}_{0.98}\text{Mg}_{0.02}\text{O}_3$ ,  $\text{LaCo}_{0.95}\text{Mg}_{0.05}\text{O}_3$ , and  $\text{La}_{0.99}\text{Sr}_{0.01}\text{CoO}_3$  (not shown in Fig. 3) is related to the concentration of mobile holes  $n_h = 0.01/\text{Co}$ , deduced from the thermopower plateaux, one gets an estimation for size of the magnetic polarons,  $S = 7-10$ . (In our previous short communication on  $\text{LaCo}_{0.95}\text{M}_{0.05}\text{O}_3$  systems, the Curie term was related to total doping  $n = 0.05$  so that smaller  $S = 2-3$  was deduced.<sup>19</sup>) It is worth mentioning that magnetic species of the same value  $S = 7-10$  were evidenced earlier in lightly doped  $\text{La}_{1-x}\text{Sr}_x\text{CoO}_3$  ( $x = 0.001-0.010$ ) using Brillouin fits of magnetization curves at temperatures down to 2 K.<sup>20</sup>

The cobaltites  $\text{LaCo}_{1-x}\text{Ti}_x\text{O}_3$  are examples of less common  $\text{Co}^{3+}/\text{Co}^{2+}$  perovskites. Previous works report on possibility of  $\text{Ti}^{4+}$  substitutions up to  $x = 0.50$  and show that the highly doped compounds are strongly resistive.<sup>21</sup> Much more interest thus represent the present lightly doped systems  $\text{LaCo}_{0.98}\text{Ti}_{0.02}\text{O}_3$  and  $\text{LaCo}_{0.95}\text{Ti}_{0.05}\text{O}_3$ . Their electric transport data, plotted in Fig. 4, show that the low-temperature resistivities are considerably higher than observed in the  $\text{Mg}^{2+}$ -substituted  $\text{Co}^{3+}/\text{Co}^{4+}$  compounds, which means that the electron ( $\text{Co}^{2+}$  hopping) mobility  $\mu_e$  is two orders lower than the hole ( $\text{Co}^{4+}$  hopping) mobility  $\mu_h$  for comparable dopings. The interesting feature of the  $\text{Ti}^{4+}$ -doped samples is the linear dependence of apparent activation energy in the low-temperature region,  $E_A = \nu kT$ , shown in the inset of upper panel of Fig. 4. This observation points to a non-Arrhenius behavior of the conduction, where activation energy defined as  $E_A = k \cdot d(\ln \rho) / d(1/T)$  loses physical

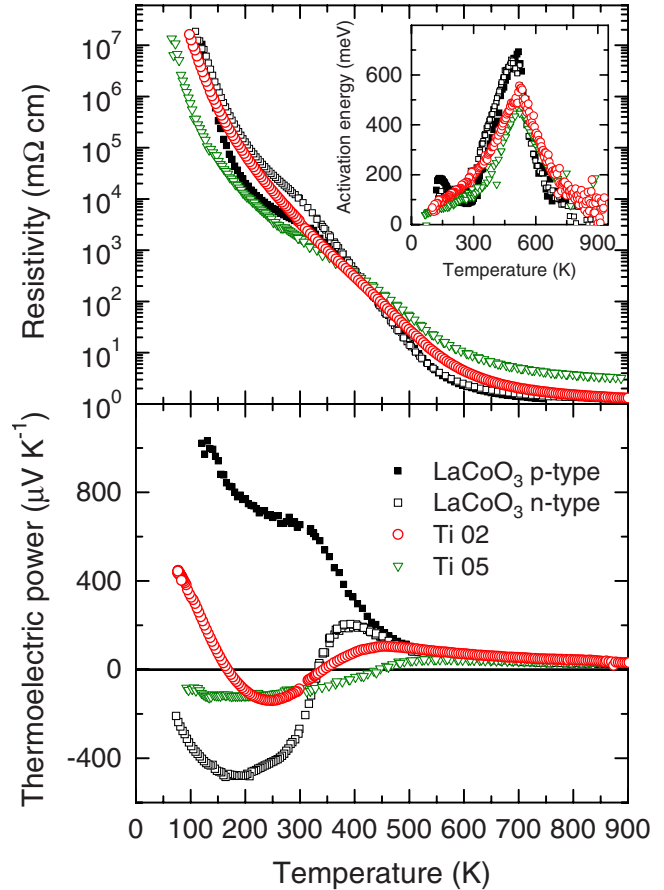


FIG. 4. (Color online) Electric resistivity and thermopower for  $n$ -type  $\text{LaCoO}_3$ ,  $\text{LaCo}_{0.98}\text{Ti}_{0.02}\text{O}_3$ ,  $\text{LaCo}_{0.95}\text{Ti}_{0.05}\text{O}_3$ . The data for  $p$ -type  $\text{LaCoO}_3$  are added for comparison

meaning. The observed behavior will be discussed in more detail below.

In Fig. 4 we include also a rather exceptional case of the  $n$ -type  $\text{LaCoO}_3$ . It is seen that the low-temperature thermopower is negative with a maximum of about  $\alpha \sim -500 \mu\text{VK}^{-1}$  at 180 K. Below this temperature, a steep turn-up to zero is observed, which suggests that the heavy  $n$ -type carriers (formally  $\text{Co}^{2+}$ ) are trapped at lower temperatures, and the conduction occurs by the very minority  $p$ -type carriers only. The presence of two types of carriers is still more evident in samples  $\text{LaCo}_{1-x}\text{Ti}_x\text{O}_3$ , where  $\text{Ti}^{4+}$  doping generates additional electron carriers in the Co-O subsystem. This is most markedly seen by the thermopower behavior for  $x = 0.02$ , where a negative maximum of  $\alpha \sim -150 \mu\text{VK}^{-1}$  is achieved at 250 K and on cooling, the thermopower crosses zero at 170 K and increases steeply to large positive values ( $\alpha_{100\text{K}} \sim +400 \mu\text{VK}^{-1}$  at 80 K). The  $x = 0.05$  sample displays a plateau of  $\alpha \sim -120 \mu\text{VK}^{-1}$  at 150–350 K. Considering  $n$ -type carriers only and applying Heikes formula, this value would lead to an unrealistic estimate of  $n_e \sim 0.20/\text{Co}$ . Consequently, the two-type charge carriers should be again anticipated. For such case of nonrecombining  $n$ - and  $p$ -type hopping carriers in the system, two contributions of opposite polarity should be combined:



$$\alpha = (n_h \cdot \mu_h \cdot \alpha_h + n_e \cdot \mu_e \cdot \alpha_e) / (n_h \cdot \mu_h + n_e \cdot \mu_e),$$

where  $\alpha_{h,e} = \pm (k/e) \ln\{(1-n_{h,e})/n_{h,e}\}$  are the Heikes thermopower terms and  $\mu_h, \mu_e$  are mobilities for the  $p$ - and  $n$ -type carriers, respectively. One may suppose that  $n_h \leq 0.001/\text{Co}$  so that  $n_e \gg n_h$  and, consequently,  $\alpha_h > -\alpha_e$  in  $\text{LaCo}_{0.98}\text{Ti}_{0.02}\text{O}_3$  and  $\text{LaCo}_{0.95}\text{Ti}_{0.05}\text{O}_3$ . The smaller contribution to the thermoelectric power of minor carriers might be, however, compensated by their higher itinerancy at the lowest temperatures. The temperature dependence of the resulting thermopower is thus controlled by an interplay of the carrier concentrations and mobilities.

Just above the room temperature, both the  $n$ -type  $\text{LaCoO}_3$  and  $\text{LaCo}_{1-x}\text{Ti}_x\text{O}_3$  sample with  $x=0.02$  quickly revert to the  $p$ -type conductor as a result of massive population of hole carriers in the course of the I-M transition. For sample  $x=0.05$ , this crossover is shifted to 450 K. The I-M transitions are practically identical for  $n$ - and  $p$ -type  $\text{LaCoO}_3$ , and both Ti-doped samples except for some effects of Co site disorder in latter compounds.

The magnetic susceptibility of  $\text{LaCo}_{0.98}\text{Ti}_{0.02}\text{O}_3$  and  $\text{LaCo}_{0.95}\text{Ti}_{0.05}\text{O}_3$  (see Fig. 3) shows a presence of Curie-type contribution of comparable value to analogously doped samples  $\text{LaCo}_{1-x}\text{Mg}_x\text{O}_3$ . This observation points to an existence of the large spin polarons also for the  $n$ -type cobaltites.

### B. The hole- and electron-doped systems $\text{DyCo}_{1-x}\text{M}_x\text{O}_3$ , $M=\text{Mg}^{2+}$ , and $\text{Ti}^{4+}$

The main distinction between the La- and Dy-based cobaltites is the extension of the LS phase stability in  $\text{DyCoO}_3$  well above the room temperature. The diamagnetism of  $\text{Co}^{3+}$  ions is, however, obscured by very strong paramagnetic contribution from Dy moments, which does not allow to determine what is the eventual magnetic effect of carriers introduced by the  $\text{Mg}^{2+}$  or  $\text{Ti}^{4+}$  doping on Co sites.

The transport data in Fig. 5 reveal much larger resistivity values compared to the  $\text{LaCo}_{1-x}\text{M}_x\text{O}_3$  systems—three orders of magnitude higher at room temperature and below, and about one order higher at temperatures close to 800–900 K. The resistivity transition is centered at  $\sim 700$  K, somewhat below  $T_{I-M}=780$  K derived from the anomalous expansion experiments.<sup>17</sup> The low-temperature conductivity in the pure  $\text{DyCoO}_3$  and  $\text{DyCo}_{0.98}\text{Mg}_{0.02}\text{O}_3$  is of Arrhenius type as shown by the activation energy in the inset of Fig. 5, which attains a large value at 200 K ( $E_A \sim 300$  meV) and slowly decreases toward 400 K. The samples show also markedly higher thermopower values compared to analogous La-based compounds. Moreover, no obvious plateaux is achieved with increasing temperature for  $\text{Mg}^{2+}$  doping, which suggests that extra charges ( $\text{Co}^{4+}$ ) are trapped in the diamagnetic cobalt sublattice and require thermal activation to be released.

The transport data for two  $\text{Ti}^{4+}$ -doped samples ( $\text{DyCo}_{0.98}\text{Ti}_{0.02}\text{O}_3$  and  $\text{DyCo}_{0.95}\text{Ti}_{0.05}\text{O}_3$ ) are remarkably similar. The conductivity up to 450 K is of non-Arrhenius type and is manifested in the inset of Fig. 5 by analogous linear dependence of apparent activation energy as evidenced above for the  $\text{LaCo}_{1-x}\text{Ti}_x\text{O}_3$  systems. The thermopower coefficient is negative below 380–400 K, pointing to a dominating role of the  $n$ -type carriers ( $\text{Co}^{2+}$  ions). It falls quickly

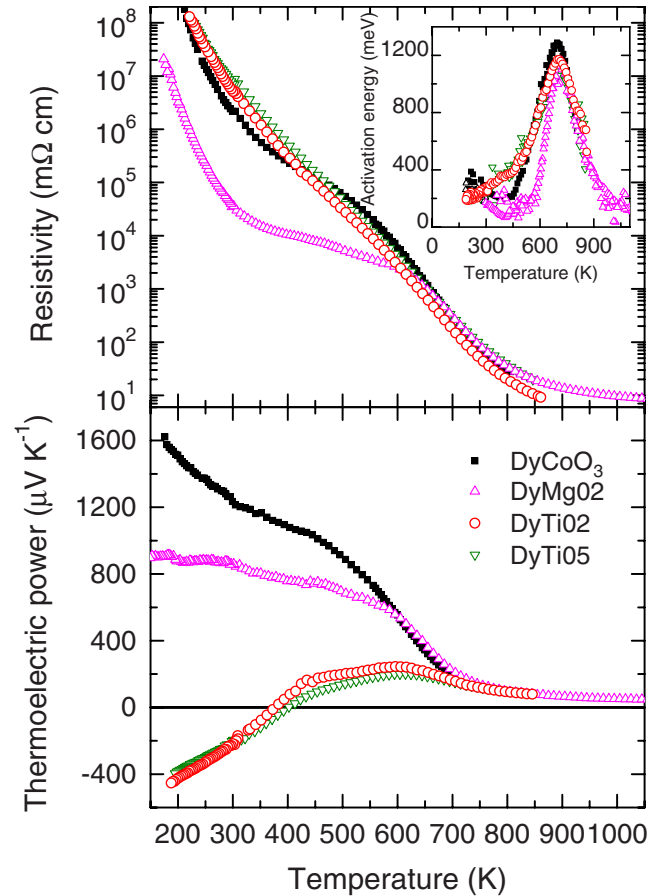


FIG. 5. (Color online) Electric resistivity and thermopower for  $\text{DyCo}_{1-x}\text{M}_x\text{O}_3$ ,  $M=\text{Mg}^{2+}$ ,  $\text{Ti}^{4+}$  systems.

with decreasing temperature to  $\alpha_{200\text{K}} \sim -400 \mu\text{V/K}$  and is immeasurable below 200 K where resistivity exceeds  $\rho \sim 10^5 \Omega \text{ cm}$ . The positive thermopower in the Ti-doped samples above 400 K can be associated with the thermal population of  $p$ -type carriers and with the onset of I-M transition (see the inset of upper panel of Fig. 5). The thermopower curves fuse with data on pure  $\text{DyCoO}_3$  at 700 K, i.e., at the point where the I-M transition culminates.

## IV. DISCUSSION

The  $\text{LnCoO}_3$  cobaltites are diamagnetic at low temperatures and undergo with increasing temperature two successive transitions. In the present interpretation, the transitions are associated with a change of local  $\text{Co}^{3+}$  spin states from LS ground state to close-lying HS and more distant IS excited states. Recent LDA+U calculations for dilute HS or IS states in the LS matrix show that the HS states prefer to be correlated by the diamagnetic LS states, and their magnetic interactions are effectively of the AFM type (in accordance with Fig. 1), while the IS states tend to coagulate and exhibit FM correlations.<sup>22</sup> The actual statistics depends on how the pair correlations and lattice expansion effects are treated—excitation energies  $\Delta_1 \sim 0.014$  eV (LS  $\rightarrow$  HS) and  $\Delta_2 \sim 0.220$  eV (LS  $\rightarrow$  IS) have been found in a fit of anomalous expansion data of  $\text{LaCoO}_3$  in our previous paper.<sup>23</sup> An alter-

native thermodynamic model using the same LS  $\rightarrow$  HS  $\rightarrow$  IS scenario has been reported by Kyömen *et al.*<sup>24</sup>

The values  $\Delta_1 \sim 0.014$  eV,  $\Delta_2 \sim 0.220$  eV are consistent with energy level diagram of CoO<sub>6</sub> cluster, calculated for LaCoO<sub>3</sub> within full atomic multiplet theory including the hybridization with oxygen 2p ligands—see Fig. 2 in Ref. 10. This cluster calculation also demonstrates that the IS Co<sup>3+</sup> state at energy  $\Delta_2$  corresponds to an electronic  $t_{2g}^5 e_g^1$  configuration in which the  $d_{x^2-y^2}$  electron is combined with the  $d_{xy}$  hole. This particular combination is more susceptible to the spin-orbit coupling than to any Jahn-Teller effects, so that observation of local distortions in Ref. 5 need not to be evidence for IS states below the room temperature.

With increasing  $Ln$  size the LS ground state is stabilized rapidly. The expected excitation energies for DyCoO<sub>3</sub> should be close to those determined for YCoO<sub>3</sub>— $\Delta_1 \sim 0.2$  eV,  $\Delta_2 \sim 0.3$  eV.<sup>18</sup>

As concerns the electrical properties, the band structure calculations show that the ideal Co<sup>3+</sup> systems  $LnCoO_3$  in their LS ground state are insulators with charge gap of about 1.0 eV. In LaCoO<sub>3</sub>, the local excitation of HS states starts at  $\sim 40$  K and it is practically accomplished at 150 K. The room-temperature paramagnetic phase is stabilized as a dynamic equilibrium of LS/HS states close to the 1:1 ratio. Such equilibrium presumes a kind of real electron exchange between Co neighbors. The band structure calculations suggest that this exchange occurs via  $t_{2g}$  channel (the calculated charge transfer gap  $\sim 0.7$  eV), in particular through a charge excitation reaction  $LS\ Co^{3+}(t_{2g}^6 e_g^0) + HS\ Co^{3+}(t_{2g}^4 e_g^2) \rightarrow LS\ Co^{4+}(t_{2g}^5 e_g^0) + HS\ Co^{2+}(t_{2g}^5 e_g^2)$ .<sup>13</sup> The reverse process, charge equalization, may occur through both the  $t_{2g}$  and  $e_g$  channels, where the latter one results at elevated temperatures in increasing population of IS Co<sup>3+</sup> pairs due to reaction  $LS\ Co^{4+}(t_{2g}^5 e_g^0) + HS\ Co^{2+}(t_{2g}^5 e_g^2) \rightarrow 2\ IS\ Co^{3+}(t_{2g}^5 e_g^1)$ . The right-hand pairs coagulate because of strong attraction between the IS Co<sup>3+</sup> states, leading at about 500 K to thermally stable IS domains of metallic character that coexist with residual semiconducting LS/HS regions. Such phase separation is responsible for rather poor macroscopic conduction, reflected in the high-temperature resistivity and thermopower, which are distinct from typical metallic behavior encountered in La<sub>1-x</sub>Sr<sub>x</sub>CoO<sub>3</sub> in the region  $x > 0.2$ .<sup>25</sup>

In cobaltites with smaller rare-earth cation, the saturation of LS/HS states close to the 1:1 ratio is not achieved because the IS states develop concurrently, but the same mechanism of the charge excitation and stabilization of the metallic IS phase can be anticipated.

The main experiments presented in this paper concern the properties of LaCoO<sub>3</sub> and DyCoO<sub>3</sub> cobaltites upon the introduction of extra hole or electron carriers by chemical substitution on Co sites by heterovalent Mg<sup>2+</sup> and Ti<sup>4+</sup> ions. The magnetic susceptibility of the LaCoO<sub>3</sub>-derived systems combined with thermopower data shows that itinerant carriers of both the  $p$  and  $n$  type form magnetic polarons of large total spin, which are thermally stable below  $T_{I-M}$ , i.e., before they are dissolved in the bulk IS phase. This finding is in agreement with previous reports on magnetic polarons in lightly doped La<sub>1-x</sub>Sr<sub>x</sub>CoO<sub>3</sub>, based on the neutron spectroscopy and diffraction experiments.<sup>26,27</sup> As pointed out by Yamaguchi *et al.*,<sup>20</sup> the observed large spin species may arise due to delo-

calization of an extra hole of mixed Co3d-O2p character over a cluster, including central cobalt ion and its close neighbors. The polaron in the hole-doped system can be thus viewed as a droplet of the metallic phase known for La<sub>1-x</sub>Sr<sub>x</sub>CoO<sub>3</sub> ( $x > 0.2$ )—see also Phelan *et al.*<sup>27</sup> In the case of electron-doped system, the double-exchange-like mechanisms can be envisaged for the magnetic polaron formation.

The magnetic polarons induced by the light doping move in seemingly unperturbed background of undoped LaCoO<sub>3</sub>, making the LS and mixed LS+HS phases semiconducting. As concerns the dynamic behavior of the polaronic carriers, it is worth mentioning that results obtained on the compound LaCo<sub>0.95</sub>Ga<sub>0.05</sub>O<sub>3</sub> differ only little from pure LaCoO<sub>3</sub>. This shows that the static disorder caused by isovalent Ga<sup>3+</sup> substitution in Co sites does not change the character of electric transport. The Mg<sup>2+</sup> doped samples are formal analogs of lightly doped La<sub>1-x</sub>Sr<sub>x</sub>CoO<sub>3</sub> compounds. Nevertheless, the transport and magnetic properties suggest that number of mobile carriers is limited to about  $n_h \sim 0.01/\text{Co}$  irrespective the actual doping. The mobility of carriers (large spin polarons) is characterized by activation energy that is maximal at an early stage of the HS excitation and amounts to 50 and 250 meV for the LaCoO<sub>3</sub>- and DyCoO<sub>3</sub>-derived systems, respectively. The activation energy decreases at higher temperatures. This easier electrical transport with increasing HS population in the LaCoO<sub>3</sub> background can be understood considering the IS nature of the polarons. Namely, the polaron diffusion involves necessarily a mechanism of formation of new IS states, which is likely related to the above-mentioned excitation reaction of the LS+HS Co<sup>3+</sup> pairs.

Properties of Ti<sup>4+</sup>-doped samples are more complex and the question on character of the charge carriers remains still open. The expected  $n$  type is supported by the negative thermopower observed at low temperatures in the lightly doped samples. No marked thermopower anomaly is observed upon the transition to the LS/HS phase while the conductivity steadily increases. This proves that carriers are not associated with bare LS Co<sup>2+</sup> ( $t_{2g}^6 e_g^1$ ) states since these are able to hop over the LS Co<sup>3+</sup> ( $t_{2g}^6 e_g^0$ ) sites only and would be strongly scattered by the HS Co<sup>3+</sup> ( $t_{2g}^4 e_g^2$ ) states. The increasing conductivity is thus another argument that the carriers form large spin polarons.

With increasing temperature and massive population of thermally induced holes, the transport properties the lightly Ti<sup>4+</sup>-doped samples approach those for pure LaCoO<sub>3</sub> and DyCoO<sub>3</sub>. We note, finally, that the large spin polarons seem to be absent in samples with higher Ti<sup>4+</sup> substitutions, presumably due to formation of more stable HS Co<sup>2+</sup> ( $t_{2g}^5 e_g^2$ ) states. In particular for LaCo<sub>1-x</sub>Ti<sub>x</sub>O<sub>3</sub> with  $x \geq 0.10$ , a positive thermopower is reported in the whole low-temperature region, pointing that the semiconducting properties are associated with minor hole carriers present in the Co sublattice extrinsically.

A special attention deserves the behavior of electric conductivity in the Ti<sup>4+</sup> lightly doped samples in the lower temperature range before the I-M transition starts. The transport observed in LaCo<sub>1-x</sub>Ti<sub>x</sub>O<sub>3</sub> up to 300 K and DyCo<sub>1-x</sub>Ti<sub>x</sub>O<sub>3</sub> up to 450 K is thermally activated but differs in the temperature dependence from the Mg<sup>2+</sup>-doped samples. This is shown in more detail in Fig. 6 (upper panel), where a plot of apparent

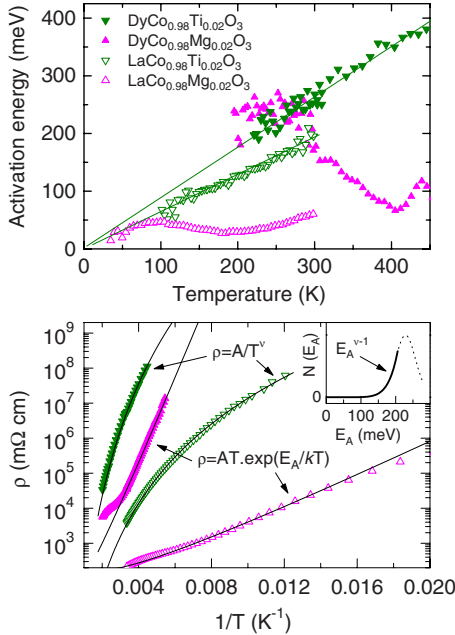


FIG. 6. (Color online) The resistivity in  $\text{LaCo}_{0.98}\text{M}_{0.02}\text{O}_3$  ( $T < 300$  K) and  $\text{DyCo}_{0.98}\text{M}_{0.02}\text{O}_3$  ( $T < 450$  K), where  $M = \text{Mg}^{2+}$ ,  $\text{Ti}^{4+}$ . The upper panel shows the linear dependence of an apparent activation energy in  $\text{Ti}^{4+}$ -doped systems  $E_A = \nu kT$ , compared to distinct dependence for the  $\text{Mg}^{2+}$  doped systems. The lower plot of  $\rho$  vs  $1/T$  demonstrates the simple Arrhenius-type behavior for the  $\text{Mg}^{2+}$  doping, while the data for the  $\text{Ti}^{4+}$  doping are fitted by a power law dependence  $\rho \sim 1/T^\nu$  ( $\nu = 8$  and  $10$ ). The distribution of hopping barriers that may explain such dependence is schematically shown in the inset (for details see the text).

activation energies  $E_A = k \cdot d(\ln \rho) / d(1/T)$  demonstrates an unusual linear dependence  $E_A = \nu kT$  with  $\nu = 8$  and  $10$  for the La- and Dy-derived samples, respectively. This finding means that the temperature dependence of bulk conductivity in the  $\text{Ti}^{4+}$ -doped cobaltites is in fact close to a power law character,  $\rho \sim 1/T^\nu$ . To demonstrate different behavior for the  $\text{Mg}^{2+}$ - and  $\text{Ti}^{4+}$ -doped samples, the observed resistivity is plotted vs  $1/T$  in the lower panel of Fig. 6. The non-Arrhenius character in the  $\text{Ti}^{4+}$ -doped cobaltites ( $x = 0.02, 0.05$ ), manifested by the pronounced curvature, might be a more general phenomenon, which we relate to a presence of intrinsic disorder on the mesoscopic scale. The conduction can be modeled as hopping of carriers over barriers of variable heights, see, e.g., Ref. 28. Our simulation of the observed power law dependence suggests that the distribution of barrier heights should have broad tail in a specific form  $N(E_A) \sim E_A^{\nu-1}$ , extending from  $E \cong 0$  to  $E_A \gg kT_{\text{max}}$  ( $T_{\text{max}} = 300\text{--}450$  K for the present  $\text{Ti}^{4+}$ -doped samples). The distribution that may explain the power law dependence observed for  $\text{LaCo}_{0.98}\text{Ti}_{0.02}\text{O}_3$  is illustrated in the inset of lower panel of Fig. 6. Only the hopping paths over barriers  $E_A$

$= 0\text{--}200$  meV (the solid line) contribute to the bulk conductivity in the range up to 300 K. With further temperature increase, other paths become accessible and the calculated conductivity will gradually tend to the standard Arrhenius behavior.

## V. CONCLUSIONS

The  $\text{LnCoO}_3$  perovskites exhibit an insulating ground state based on the diamagnetic LS  $\text{Co}^{3+}$ . The transition to the paramagnetic state is interpreted on a basis of the LS  $\rightarrow$  HS  $\text{Co}^{3+}$  local excitation, which is followed at higher temperature by formation of the metallic IS phase through a charge transfer mechanism between LS/HS pairs. In  $\text{LaCoO}_3$ , the LS  $\rightarrow$  HS excitation rate is fastest at  $T_{\text{magn}} = 80$  K and practically saturates for  $T > 150$  K, where HS to LS ratio approaches 1. The second transition is centered at  $T_{I-M} = 540$  K. On the other hand, the transitions in  $\text{DyCoO}_3$  proceed nearly concurrently ( $T_{\text{magn}} = 740$  K and  $T_{I-M} = 780$  K). It is pointed out that the interactions in the mixed LS/HS phase prevent HS  $\text{Co}^{3+}$  states to be stabilized at the nearest neighbor sites, while IS  $\text{Co}^{3+}$  states show an opposite tendency and prefer clustering. This makes a condition for an intrinsically phase-separated state above  $T_{I-M}$ , where the metallic IS domains coexist with residual LS/HS regions.

The experimental results on electrical resistivity and thermopower, complemented with magnetic data, suggest that each hole and electron carrier, present in  $\text{LaCoO}_3$  and  $\text{DyCoO}_3$  due to nonstoichiometry or light doping on  $\text{Co}^{3+}$  sites with  $\text{Mg}^{2+}$  and  $\text{Ti}^{4+}$ , is associated with magnetic polaron of large spin value  $S = 7\text{--}10$ . This polaron can be viewed as a droplet of metallic phase, analogous to the IS phase that is induced in  $\text{LaCoO}_3$  by a high-temperature activation or is realized as the ferromagnetic ground state in  $\text{La}_{1-x}\text{Sr}_x\text{CoO}_3$  for  $x > 0.2$ . The existence of the large spin polarons is thus a key for understanding of the whole  $(x, T)$  phase diagram of the cobaltites.

At temperatures below  $T \sim 300$  K and 450 K for  $\text{LaCoO}_3$  and  $\text{DyCoO}_3$ , respectively, the magnetic polarons move in the background of  $\text{Co}^{3+}$  sites in LS or mixed LS/HS states. The conductivity is of strongly activated type for both the  $p$ - and  $n$ -type systems. However, a clearly non-Arrhenius behavior is detected in the  $n$ -type ( $\text{Ti}^{4+}$ -doped) compounds, deviating significantly from standard dependence  $\rho \sim \exp(E_A/kT)$  and also from Mott's formula for "variable range hopping." In the mentioned temperature region, the observed resistivity follows a simple power law formula  $\rho \sim 1/T^\nu$  ( $\nu = 8\text{--}10$ ).

## ACKNOWLEDGMENTS

The work was supported by Grant No. A100100611 of the Grant Agency of the Academy of Sciences of the Czech Republic.

- <sup>1</sup>R. R. Heikes, R. C. Miller, and R. Mazelsky, *Physica* (Amsterdam) **30**, 1600 (1964).
- <sup>2</sup>P. M. Raccach and J. B. Goodenough, *Phys. Rev.* **155**, 932 (1967).
- <sup>3</sup>K. Asai, A. Yoneda, O. Yokokura, J. M. Tranquada, G. Shirane, and K. Kohn, *J. Phys. Soc. Jpn.* **67**, 290 (1998).
- <sup>4</sup>D. P. Kozlenko, N. O. Golosova, Z. Jirak, L. S. Dubrovinsky, B. N. Savenko, M. G. Tucker, Y. Le Godec, and V. P. Glazkov, *Phys. Rev. B* **75**, 064422 (2007).
- <sup>5</sup>G. Maris, Y. Ren, V. Volotchaev, C. Zobel, T. Lorenz, and T. T. M. Palstra, *Phys. Rev. B* **67**, 224423 (2003); D. Louca and J. L. Sarrao, *Phys. Rev. Lett.* **91**, 155501 (2003); A. Ishikawa, J. Nohara, and S. Sugai, *ibid.* **93**, 136401 (2004); S. K. Pandey, S. Khalid, N. P. Lalla, and A. V. Pimpale, *J. Phys.: Condens. Matter* **18**, 10617 (2006).
- <sup>6</sup>V. P. Plakhty, P. J. Brown, B. Grenier, S. V. Shiryayev, S. N. Barilo, S. V. Gavrilov, and E. Ressouche, *J. Phys.: Condens. Matter* **18**, 3517 (2006).
- <sup>7</sup>S. K. Pandey, A. Kumar, S. Patil, V. R. R. Medicherla, R. S. Singh, K. Maiti, D. Prabhakaran, A. T. Boothroyd, and A. V. Pimpale, *Phys. Rev. B* **77**, 045123 (2008); R. F. Klie, J. C. Zheng, Y. Zhu, M. Varela, J. Wu, and C. Leighton, *Phys. Rev. Lett.* **99**, 047203 (2007), and references therein.
- <sup>8</sup>S. Noguchi, S. Kawamata, K. Okuda, H. Nojiri, and M. Motokawa, *Phys. Rev. B* **66**, 094404 (2002).
- <sup>9</sup>Z. Ropka and R. J. Radwanski, *Phys. Rev. B* **67**, 172401 (2003).
- <sup>10</sup>M. W. Haverkort, Z. Hu, J. C. Cezar, T. Burnus, H. Hartmann, M. Reuther, C. Zobel, T. Lorenz, A. Tanaka, N. B. Brookes, H. H. Hsieh, H.-J. Lin, C. T. Chen, and L. H. Tjeng, *Phys. Rev. Lett.* **97**, 176405 (2006).
- <sup>11</sup>A. Podlesnyak, S. Streule, J. Mesot, M. Medarde, E. Pomjakushina, K. Conder, A. Tanaka, M. W. Haverkort, and D. I. Khomskii, *Phys. Rev. Lett.* **97**, 247208 (2006).
- <sup>12</sup>M. Zhuang, W. Zhang, and N. Ming, *Phys. Rev. B* **57**, 10705 (1998).
- <sup>13</sup>K. Knizek, Z. Jirak, J. Hejtmanek, and P. Novak, *J. Phys.: Condens. Matter* **18**, 3285 (2006).
- <sup>14</sup>M. A. Señarís-Rodríguez and J. B. Goodenough, *J. Solid State Chem.* **116**, 224 (1995).
- <sup>15</sup>C. Zobel, M. Kriener, D. Bruns, J. Baier, M. Grüninger, T. Lorenz, P. Reutler, and A. Revcolevschi, *Phys. Rev. B* **66**, 020402(R) (2002).
- <sup>16</sup>J. Hejtmanek (unpublished).
- <sup>17</sup>K. Knizek, Z. Jirak, J. Hejtmanek, M. Veverka, M. Marysko, G. Maris, and T. T. M. Palstra, *Eur. Phys. J. B* **47**, 213 (2005).
- <sup>18</sup>Y. Tokura, Y. Okimoto, S. Yamaguchi, H. Taniguchi, T. Kimura, and H. Takagi, *Phys. Rev. B* **58**, R1699 (1998).
- <sup>19</sup>J. Hejtmanek, Z. Jirak, K. Knizek, M. Marysko, M. Veverka, and C. Autret, *J. Magn. Magn. Mater.* **320**, e92 (2008).
- <sup>20</sup>S. Yamaguchi, Y. Okimoto, H. Taniguchi, and Y. Tokura, *Phys. Rev. B* **53**, R2926 (1996).
- <sup>21</sup>R. Robert, L. Bocher, M. Trottmann, A. Reller, and A. Weidenkaff, *J. Solid State Chem.* **179**, 3893 (2006); D. L. Cairns, I. M. Reaney, H. Zheng, D. Iddles, and T. Price, *J. Eur. Ceram. Soc.* **25**, 433 (2005).
- <sup>22</sup>K. Knizek, Z. Jirak, J. Hejtmanek, P. Novak, and W. Ku (unpublished).
- <sup>23</sup>K. Knizek, Z. Jirak, J. Hejtmanek, P. Henry, and G. André, *J. Appl. Phys.* **103**, 07B703 (2008).
- <sup>24</sup>T. Kyômen, Y. Asaka, and M. Itoh, *Phys. Rev. B* **67**, 144424 (2003).
- <sup>25</sup>Y. Kashiwada, H. Fujishiro, Y. Fujine, M. Ikebe, and J. Hejtmanek, *Physica B* (Amsterdam) **378-380**, 529 (2006).
- <sup>26</sup>A. Podlesnyak, K. Conder, E. Pomjakushina, A. Mirmelstein, P. Allenspach, and D. I. Khomskii, *J. Magn. Magn. Mater.* **310**, 1552 (2007).
- <sup>27</sup>D. Phelan, D. Louca, S. Rosenkranz, S.-H. Lee, Y. Qiu, P. J. Chupas, R. Osborn, H. Zheng, J. F. Mitchell, J. R. D. Copley, J. L. Sarrao, and Y. Moritomo, *Phys. Rev. Lett.* **96**, 027201 (2006).
- <sup>28</sup>J. M. Marshall and J. Optoelectron, *Adv. Mater. (Weinheim, Ger.)* **9**, 84 (2007).